Desalination and Water Treatment
www.deswater.com

doi: 10.5004/dwt.2019.23380

143 (2019) 38–47
March

Comparison of physical cleaning techniques for membrane distillation: temperature reversal, air sparging, and ultrasonication

Jihyeok Choi, Yongjun Choi, Yongsun Jang, Yonghyun Shin, Sangho Lee*

School of Civil and Environmental Engineering, Kookmin University, 77 Jeongneung-ro, Seoungbuk-gu, Seoul 02707, Korea, Tel. +82 2 910 4529; Fax: +82 2 910 4529; email: sanghlee@kookmin.ac.kr (S. Lee)

Received 31 August 2018; Accepted 15 October 2018

ABSTRACT

Although membrane distillation (MD) has drawn attention as a promising thermal separation technique to produce freshwater from seawater or concentrated wastewater, membrane fouling is a critical issue to be addressed for its applications. In this study, physical cleaning techniques to mitigate fouling of MD membranes were compared, including temperature reversal, air sparging, and ultrasonication. Experiments were conducted using flat sheet polyvinylidene fluoride membranes in a bench-scale direct contact membrane distillation system. Model foulants such as silica, humic acid, and $CaSO_4$ were used to prepare feed solutions. The optimum condition for each physical cleaning technique was explored. Results showed that the air sparging was the most effective to recover flux among these three methods. The temperature reversal also showed potential to retard the progress of fouling. However, the ultrasonication does not seem to be applicable under the conditions considered in this work, because it led to severe damage of the membrane.

Keywords: Membrane distillation; Fouling; Temperature reversal; Air sparging; Ultrasonication

1. Introduction

Water shortage worldwide is facing a range of challenges caused by increasing water demand from population growth, droughts, and rising energy use from increasing uptake of energy-intensive alternative water sources [1]. Accordingly, growing requirements of freshwater is driving the interest in using renewable energy for desalination applications. Due to their less energy-intensive nature and small footprint, membrane-based desalination technologies have been gaining a significant interest [2]. Among them, membrane distillation (MD) is a thermal separation technique to produce freshwater from seawater and highly concentrated saline water. Hydrophobic membranes are used to allow the vapor pass through the membranes' pores. The driving force of the process is given by a partial vapor pressure difference commonly triggered by a temperature difference. MD has attractive advantages: (1) theoretically 100% slat rejection, (2) non-volatile species, (3) lower operation pressure than pressure-driven membrane process such as reverse osmosis, (4) reduced vapor compared with pressure-driven membrane processes, (5) lower requirements for membrane mechanical properties, and (6) its capability to use the utilization of waste heat from industrial processes of generators or renewable energy sources such as solar energy and geothermal energy [3–6].

However, major barriers against widespread use of MD are membrane wetting and fouling. Membrane wetting is a phenomenon that the pores of the membranes are filled with feedwater. This occurs when the transmembrane pressure exceeds the liquid entry pressure (LEP) of the membrane [7]. If the feedwater contains amphiphilic molecules, the hydrophobic tails of the amphiphilic molecules will attach onto the hydrophobic membrane pore surface, leading to a reduction in LEP by making the pore walls hydrophilic [8–10]. Membrane fouling is a process that the membrane surface

* Corresponding author.

or pores are blocked by contaminants, leading to a decline in the vapor flow rate through the membrane. The formation of foulant layers may also result in an increase in temperature polarization, thereby decreasing the water production by reducing driving force of separation [11]. In fact, industrial applications of MD are impeded by the lack of techniques to control membrane wetting and fouling.

A number of literatures have investigated MD fouling by various materials. The foulants found in membrane process can be divided into three broad groups according to the fouling material: inorganic fouling, organic fouling, and biological fouling [11]. It has been reported that inorganic scale-forming ions may deposit on the membrane surface and block the membrane pores, leading to a significant reduction in MD flux [12–14]. Organic materials such as humic acid (HA) have been also reported to cause MD flux by forming deposits on the upper surface of the membrane with relatively low internal fouling [15,16].

There have been a few works on the control of MD fouling by (1) developing novel membrane materials and (2) applying hydrodynamic forces by introducing aeration, flow reversal, or ultrasonic. To mitigate MD fouling, composite MD membranes were developed with a hydrophobic substrate and a hydrophilic top surface using electrospinning to mitigate oil fouling [17]. The effect of maintaining air layers on the membrane surface and superhydrophobicity was also investigated for preventing fouling of MD membranes by salts, particulates, and organic particles [18]. Moreover, flow reversal was applied to maintain high water fluxes and membrane performance [19]. In addition, ultrasonication was used for monitoring of membrane fouling monitoring, cleaning of fouled membranes, and improvement of distillate flux [20].

However, few studies have attempted to compare different techniques for MD fouling control under various conditions. Accordingly, the objective of this article was to examine the effectiveness of three physical cleaning techniques for MD fouling, including temperature reversal, air sparing, and ultrasonication. The fouling behaviors of the MD membranes were investigated using model foulants such as colloidal silica, HA, and $CaSO_4$. Then, the physical cleaning techniques were applied to the MD membranes during the fouling experiments. To the best knowledge of the authors of this article, this is the first comparative study on the physical cleaning of MD membranes by applying different techniques, which provide insight in in-depth understanding of MD fouling mechanisms and control.

2. Material and methods

2.1. Experimental materials

A hydrophobic polyvinylidene fluoride flat sheet membrane supplied by Merck Millipore Ltd. (Burlington, MA, USA, GVHP14250) was chosen to fabricate in-house membrane modules. The flat sheet membrane module was made of acrylic resin with effective depth, width, and length of 2, 20, and 60 mm, respectively. The membrane modules were designed to hold the membranes under moderate pressure differential without physical support spacer. The membrane parameters and relevant module specifications are listed in Table 1.

2.2. DCMD process

The direct contact membrane distillation (DCMD) experimental setup was used in this study as shown in Fig. 1. The temperature of feed solution was maintained constantly by a hotplate stirrer placed at bottom of the feed tank, and the thermometers were used for measuring the inlet and outlet temperature of feed and permeate flow. The permeate temperature was fixed at 20°C by flowing through heat exchanger connected with water bath. Volume of permeated water was measured by electronic balances (OHAUS), and the data were transmitted to PC during operating time. The hot feed solution and the cold distillate were supplied at constant flow rate using the two gear pumps (Cole-Parmer, Vernon Hills, IL, USA). Also, co-current flow type was employed. The flow rate was monitored using flow meters (Dywer, Michigan City, IN, USA), which was set at the inlet side of the module. The feed and permeate flow velocity were 14.58 and 8.33 cm/s, respectively, and the temperature difference (ΔT) was maintained at 40°C (feed = 60°C and permeate = 20°C). After each experiment, the membrane was dried to analyze the membrane surface.

2.3. Preparation of feed solution

Experiments were carried out to compare fouling behaviors by different types of foulants using NaCl, colloidal silica (LUDOX AM-30), HA (Sigma-Aldrich, St. Louis, MO, USA), and calcium sulfate (Sigma-Aldrich), which represents

Table 1
Summary of membrane specification

	Properties
Membrane type	Flat sheet membrane
Membrane material	Hydrophobic polyvinylidene fluoride
Pore diameter (μm)	0.22
Porosity (%)	75
Membrane of LEP (bar)	0.28
Module length (cm)	10
Effective membrane length (cm)	6
Effective membrane area (cm^2)	12

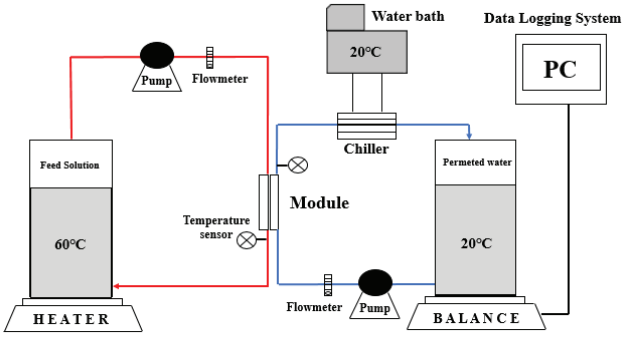

Fig. 1. Schematic diagram of laboratory-scale DCMD experimental setup.

colloidal, organic, and scale-forming foulants in natural waters, respectively [21]. The concentrations of colloidal silica, HA, and calcium sulfate were 1,000, 100, and 2,000 mg/L, respectively. In all cases, NaCl of 1,000 mg/L concentration was added to adjust the chemistry of feed solutions. The combinations of different foulants were also considered.

Table 2 summarizes the characteristics of feed solutions. They were used for the examination of MD fouling. But only E7, which contains all the foulants in the feed solution, was used in the experiments of physical cleaning.

2.4. Physical cleaning techniques

As previously mentioned, the three techniques for physical cleaning of the MD membrane were used: temperature reversal, air sparging, and ultrasonication. Schematic diagram of each cleaning method is presented in Fig. 2.

2.4.1. Temperature reversal

Temperature reversal is the effective fouling mitigation technique in MD by reversing the temperature of the feed side and the permeate side. Thus, vapor flows from distillate side to feed side, leading to the detachment of foulants from the membrane surface. Moreover, it is reported that temperature reversal is also effective in inhibiting homogeneous precipitation of salts and disrupting nucleation of sparingly soluble salts on the membrane surface [19]. In this study, temperature reversal was carried out using deionized water by adjusting the feed and permeate temperatures as shown in Fig. 2(b). It was implemented three times at the volume concentration factor (VCF) of 1.3, 1.6, and 1.9, respectively. In each case, the duration of the temperature was 1 h.

Table 2
Summary of feed solutions

Case	Feed concentration	
E1	Silica 1,000 mg/L	NaCl 1,000 mg/L
E2	HA 100 mg/L	
E3	$CaSO_4$ 2,000 mg/L	
E4	Silica 1,000 mg/L + HA 100 mg/L	
E5	$CaSO_4$ 2,000 mg/L + silica 1,000 mg/L	
E6	$CaSO_4$ 2,000 mg/L + HA 100 mg/L	
E7	Silica 1,000 mg/L + HA 100mg/L + $CaSO_4$ 2,000 mg/L	

2.4.2. Air sparging

Air sparging is a well-known technique for the control of fouling in pressure-driven membrane filtration but has not been widely applied in MD process. Air sparing has the following effects: (1) secondary flow by air bubbles, (2) physical displacement of the concentration polarization layer, (3) pressure pulsing caused by passing air bubbles, and (4) increase in superficial cross-flow velocity [11,22,23]. In this study, the air was directly injected into the feed solution using an air pump (ZP-25). The amount of air was measured using an air flowmeter, and the size of air bubbles was approximately 0.2–0.3 mm.

2.4.3. Ultrasonication

Ultrasonication is another technique to physically clean the fouled membrane. Ultrasound makes oscillating areas of high and low pressure. When pressure amplitude surpasses the tensile strength of liquid, cavitation bubbles are formed during the rarefaction of sound waves. The cavitation bubble collapses during the compression cycle of sound waves [24]. This mechanical effect promotes turbulence that reduces the temperature polarization and concentration polarization [25]. In this study, the ultrasonication was applied to the MD module that was immersed into a tank with an ultrasonic generator. The ultrasound was applied in a frequency of 40kHz and 150W in output power. Also, the ultrasound intensity range was between 20% and 100%. In order to reduce the risk of the membrane damage, ultrasound was irradiated three times during the MD experiment at VCF 1.3, 1.6, and 1.9, respectively. In each case, the duration of the temperature was 1 h.

2.5. Method

2.5.1. Experimental methods

During MD process, the feed was gradually concentrated. The degree of concentration was measured using the volume of concentration factor (VCF):

$$\mathrm{VCF}(K) = \frac{V_0}{V_0 - V_P} \tag{1}$$

where V_0 is the initial quantity of feed volume (V) and V_P is the cumulative permeate production (V). The normalized flux J_n was used to describe the ratio of flux after fouling (J) to the initial flux (J_0):

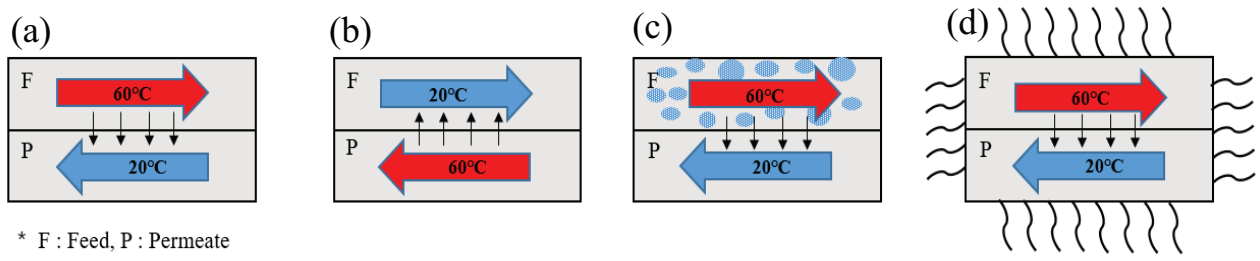

Fig. 2. (a) Basic MD operation and mechanism of physical techniques: (b) temperature reversal, (c) air sparging, and (d) ultrasonication.

$$J_n = \frac{J}{J_0} \tag{2}$$

To characterize the performance improvement achieved by physical techniques, the flux enhancement ratio Φ can be calculated:

$$\Phi = \frac{J_{p.t}}{J_{w.p.t}} \tag{3}$$

where $J_{p.t}$ and $J_{w.p.t}$ are the final permeate fluxes in the DCMD process with and without physical techniques, respectively.

2.5.2. Hermia's model

The blocking filtration models based on the Hermia's equations were used to fit the flux decline in MD process. Table 3 summarizes the Hermia's model equations and parameters [26]. Here, A is the effective area of the membrane surface, α_{block} is the measure of the pore blockage efficiency, J_0 is the initial filtrate flux through the clean membrane, and N_0 is the initial pore density. Although these models are simple, they are still widely used to evaluate the increasing behavior of filtration resistance in liquid filtration of relatively dilute suspension [26].

2.5.3. Field-emission scanning electron microscopy (FE-SEM)

The field-emission scanning electron microscopy (FE-SEM, JSM-7160F) was applied to observe the foulants on the membrane surfaces. Prior to the observations, the membrane samples were dried and mounted on the flat stubs after coated by platinum.

3. Results and discussions

3.1. Membrane fouling by single foulants

Fig. 3(a) shows the normalized flux as a function of VCF during the MD fouling experiments using single foulants. In the case of silica, stable flux was observed until VCF reached 2. However, flux decreased after the time, leading 28% of final flux reduction. It seemed that the deposition of colloidal silica particles on the surface of the membrane or within the membrane structure is regarded as the major contributor of fouling decline. Although the silica particles have negatively charged, the electrostatic interactions are weak in high ionic strength conditions [27], leading to the deposition foulants on the membrane surface.

Unlike silica, the effect of HA on flux decline was negligible. As shown in the graphs, flux did not decrease even when the feed solution was concentrated by 3.5 times. Although HA may form foulant layers on the membrane surface, it does not seem to affect the vapor transport through the membrane. Similar results were reported in a literature by Han et al. [28].

In the case of calcium sulfate, there was no change in normalized flux until induction time of VCF 1.3. However, as the feed solution was further concentrated, crystallization occurred, resulting in an abrupt flux decline. Similar results were also previously reported by Shin and Sohn [29].

After the fouling experiments, the surfaces of the membranes were examined using FE-SEM. Fig. 3(b) shows the surface of the intact membrane. Compared with this, the surfaces of the membranes after the experiments using the feed solutions were quite different. Thick cake layers were found in the case of the feed solution containing silica, as demonstrated in Fig. 3(c). The foulant layers in the case of HA have different morphologies from those in the case of silica. On the other hand, typical needle shape of calcium crystals stacked on the surfaces was observed in the case of $CaSO_4$.

Table 3
Hermia's models

Filtration model	Model equation	Model parameter
Pore blockage	$\frac{J_V}{J_O} = \exp\left(-\frac{\alpha_{block} A J_O C_b}{N_o} t\right)$	$Kt = \ln\left(\frac{J_o}{J_v}\right)$
Pore construction	$\frac{J_v}{J_o} = \left(1 + \frac{\alpha_{pore} A J_O C_b}{\pi r_o^2 \delta_m} t\right)^{-2}$	$Kt = \left(\frac{J_o}{J_v}\right)^{\frac{1}{2}} - 1$
Cake filtration	$\frac{J_v}{J_o} = \left(1 + \frac{2\alpha_{cake} J_o C_b}{R_m} t\right)^{-\frac{1}{2}}$	$Kt = \left(\frac{J_o}{J_v}\right)^{2} - 1$

3.2. Membrane fouling by feed solutions containing more than two foulants

The changes in flux during the MD experiments using feed solutions containing more than two foulants are shown in Fig. 4(a). Compared with the results in Fig. 3(a), the flux decline was mitigated in the presence of HA. In the case of silica fouling experiments, the final flux values without and with HA were 0.75 and 0.9, which corresponds to an increase by 1.2 times. In the case of $CaSO_4$ fouling experiments, the final flux values without and with HA were 0.1 and 0.8, corresponding to an increase by eight times. This is attributed to the retardation of fouling by HA adsorbed onto silica particles or $CaSO_4$ crystals. Previous works report that organic macromolecules adsorption onto active growth sites of crystals retarded gypsum scaling significantly [30].

When calcium and silica exist together in the same feed solution, the interaction between negatively charged silica and calcium cations seem to accelerate the formation of scales. This resulted in a rapid flux decline in the case of the feed containing silica and $CaSO_4$. When HA also exists in this feed solution, the fouling was slightly mitigated. But it was still serious compared with the other feed solutions.

The FE-SEM images obtained after the MD experiments are depicted in Figs. 4(b)–(e). The morphologies of the foulant layers were different from those in the cases of the single foulants. It is evident from the figures that HA affects the structures and characteristics of foulant deposits. The effect of HA on CaSO4 crystal morphology was also reported in previous work [30]. On the other hand, the addition of silica to the $CaSO_4$ solution did not significantly change the morphology of the foulant layers (Figs. 3(e) and 4(c)).

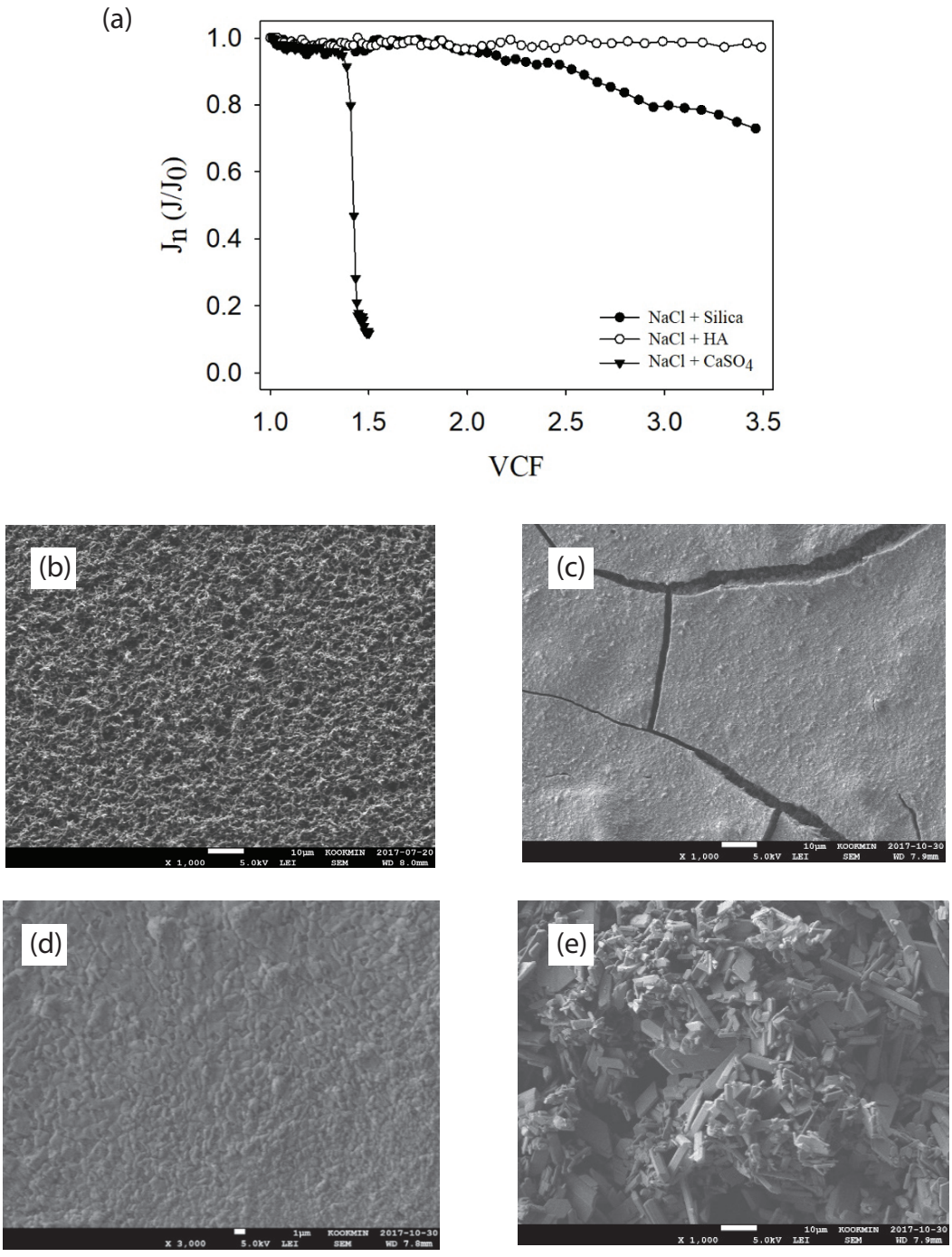

Fig. 3. (a) Effect of single foulant on normalized flux, FE-SEM images of the membrane surface: (b) clean membrane surface, (c) NaCl + silica, (d) NaCl + HA, and (e) NaCl + $CaSO_4$.

3.3. Hermia's model value of colloidal fouling

The Hermia models shown in Table 3 were applied to fit the experimental data from the case of feed solution containing silica, HA, and $CaSO_4$. The results are shown in Table 4. Because the R^2 value for the pore blockage model was the highest among the three modes, it seems that the blocking of the pores by the foulants is the dominant fouling mechanisms in this case.

3.4. Physical cleaning techniques

3.4.1. Temperature reversal

To mitigate fouling by silica, HA, and $CaSO_4$, the physical cleaning techniques were attempted. The changes in flux by applying the temperature reversal are shown in Fig. 5. Results showed that the recovery of the flux also increased as the temperature difference increased. Without the temperature reversal (Fig. 5(a)), the flux recovery was negligible. At the temperature

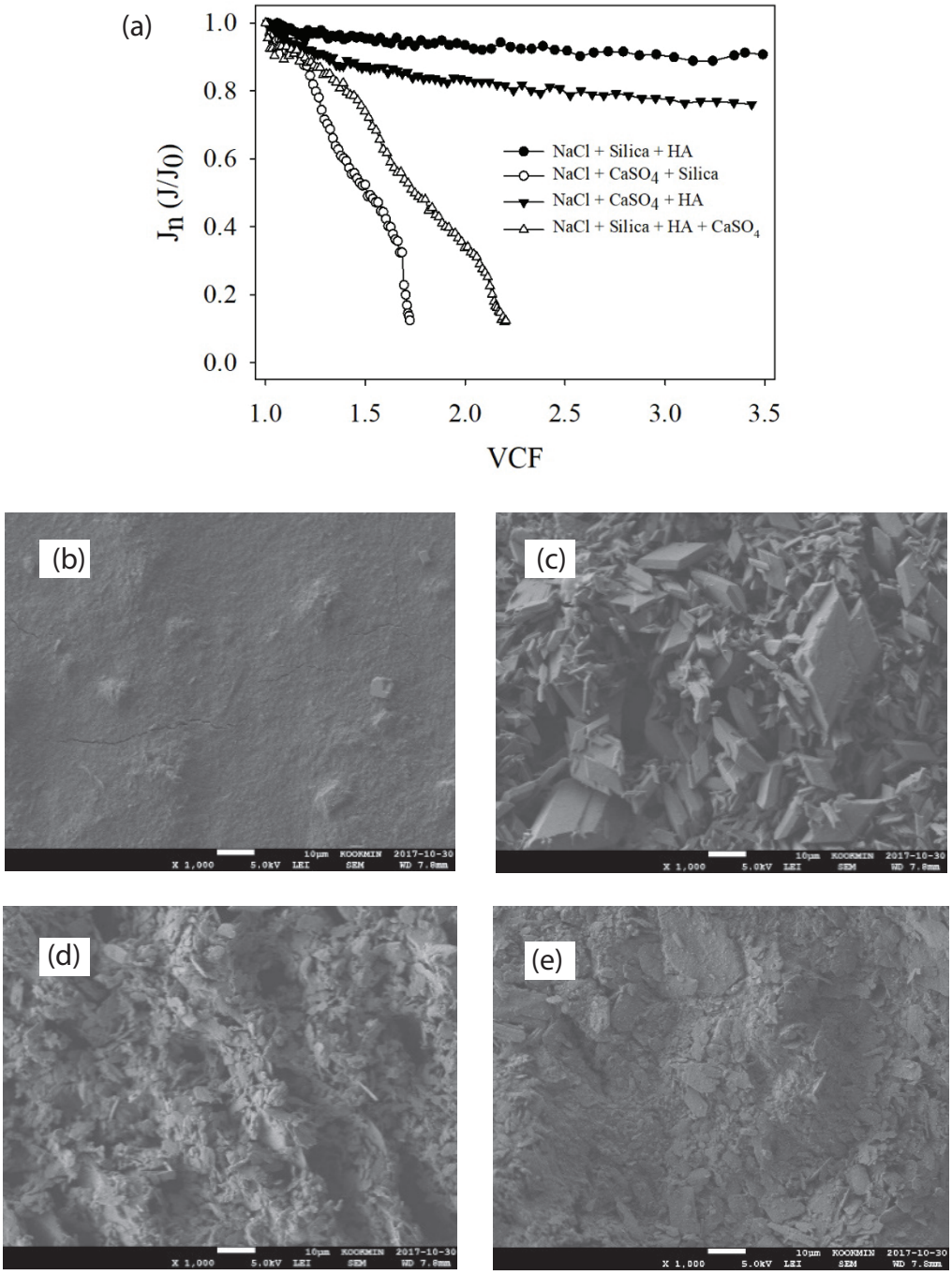

Fig. 4. (a) Effect of mixed foulants on normalized flux, FE-SEM images of the membrane surface: (b) NaCl + silica+ HA, (c) NaCl + $CaSO_4$ + silica, (d) NaCl + $CaSO_4$ + HA, and (e) NaCl + silica + HA + $CaSO_4$.

Table 4
Model parameters for the Hermia's equations in the case of feed solution containing silica, HA, and $CaSO_4$ (the case E7 in Table 2)

Filtration model	R^2	K (min^{-1})
Pore blockage	0.8827	0.00049
Pore construction	0.8294	0.00031
Cake filtration	0.6322	0.00030

difference of 30°C (Fig. 5(b)), the flux recovery ratios were 10%, 4.4%, and 4.5%, respectively. At the temperature difference of 40°C (Fig. 5(c)), they were 14.2%, 4.7%, and 4.6 %, respectively. The temperature difference of 50°C (Fig. 5(d)) resulted in the flux recovery ratios of 14.9%, 5.6%, and 4.8%, respectively. The final normalized fluxes at the temperature differences of 0, 30, 40, and 50 were 0.40, 0.44, 0.51, and 0.51, respectively. These results are attributed to the increased reverse flux with an increase in the temperature difference in the temperature reversal.

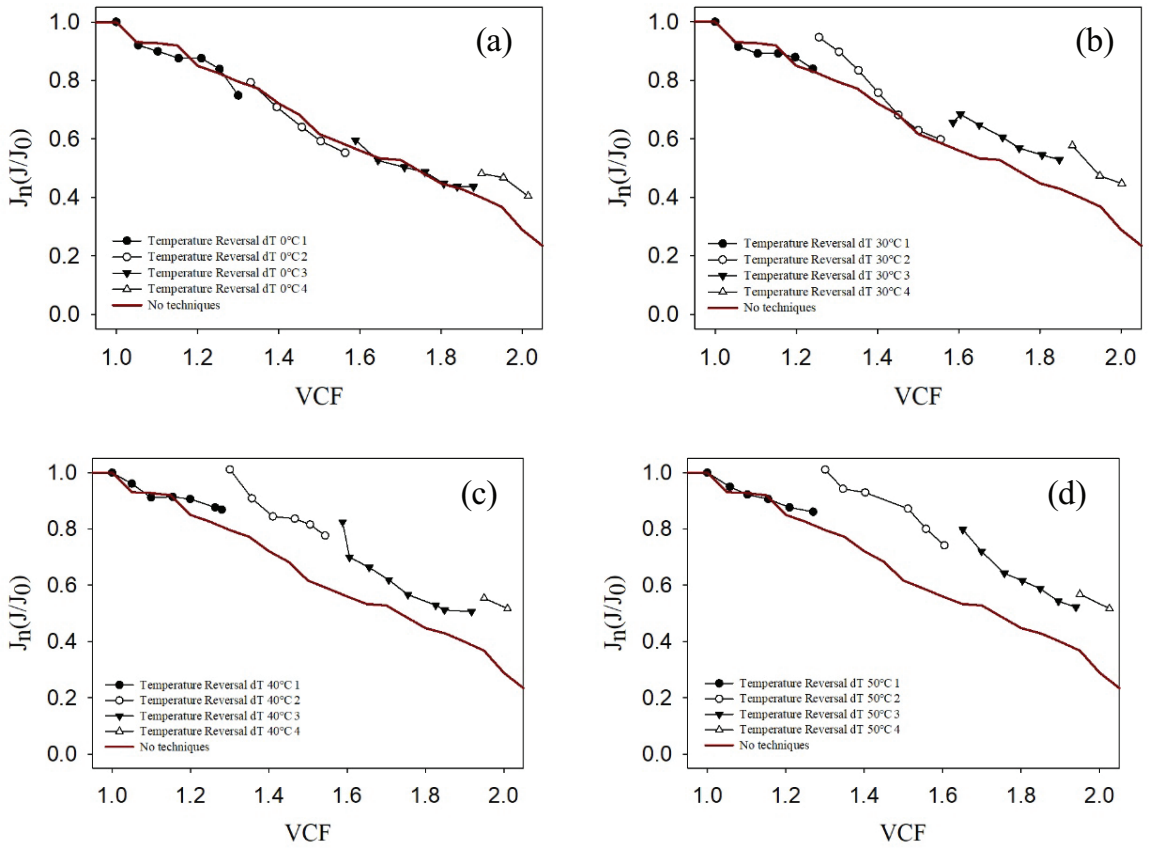

Fig. 5. Effect of temperature reversal on normalized flux under different temperature differences. (a) temperature difference of 0°C, (b) temperature difference of 30°C, (c) temperature difference of 40°C, and (d) temperature difference of 50°C.

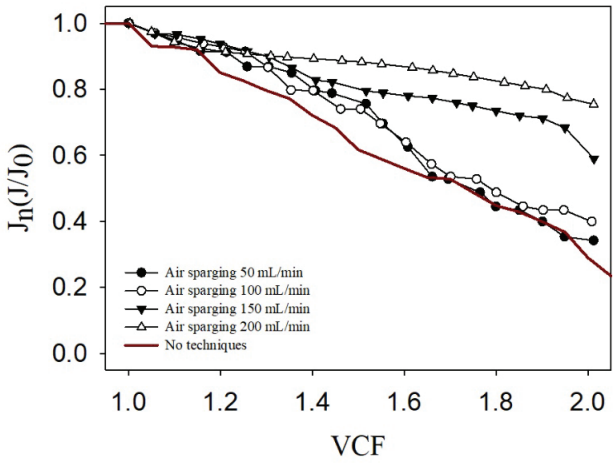

Fig. 6. Effect of air sparging on nomalized flux (conditions—air sparing rate: 50 mg/L, 100 mL/min, 150 mL/min, and 200 mL/min).

3.4.2. Air sparging

The results of air sparging during the MD experiments using the feed solution containing silica, HA, and $CaSO_4$ are shown in Fig. 6. As expected, an increase in the air sparing rate led to an enhancement of flux. When the air sparing rates were 50 mL and 100 mL/min, the final normalized flux was 0.34 and 0.39, respectively. When they were 150 mL and 200 mL/min, the final normalized flux were 0.57 and 0.75. This is attributed to the removal of foulant layers by enhanced hydrodynamic force of the air flow. The air bubbles can also result in "scouring effect" as they do in membrane bioreactors. Compared with the temperature reversal (Fig. 5(a)), the degree of flux enhancement was higher in the case of the air sparging.

The surfaces of the membranes after the applications of the temperature reversal and the air sparging are shown in Fig. 7. Compared with Fig. 4(e), which is the case without any physical cleaning, the effect of temperature reversal on the foulant layers was not clear. On the other hand, the effect of the air sparing was substantial because the structures of the intact membranes were shown. These results also support the higher efficiency of the air sparging on fouling control than that of the temperature reversal.

3.4.3. Ultrasonication

Fig. 8 shows the changes in flux with time with the application of ultrasonication. When the output power was 20%, the flux was similar to that without the ultrasonic irradiation. As the output power increased, the flux increased. At the powers of 30% and 40%, the final normalized flux was 0.40 and 0.48, respectively. At the power of 50%, the damage of the membrane was observed after the first ultrasonic irradiation. It seems that the output power of 40% was the optimum condition for ultrasonication.

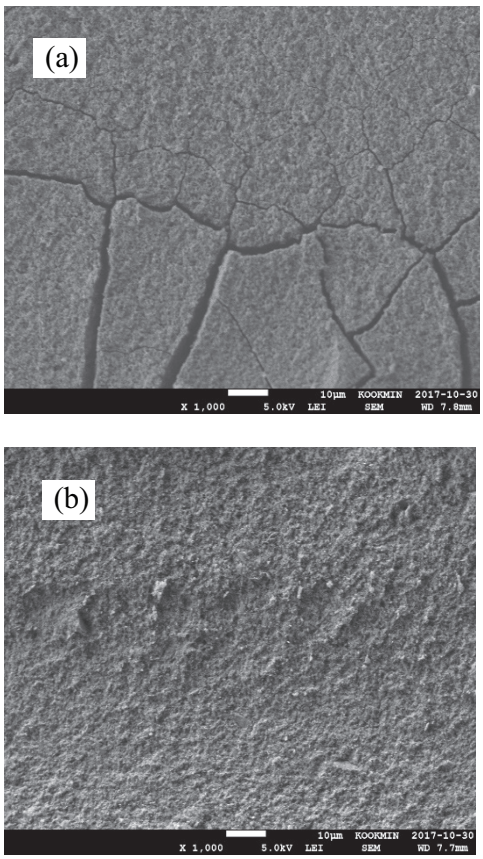

Fig. 7. Comparison of FE-SEM images of the membrane after (a) temperature reversal (ΔT: 50°C) and (b) air sparging (200 mL/min).

The damage of the membranes at high power out was also confirmed in the FE-SEM images as illustrated in Fig. 9. At the output power of 40%, the foulant surfaces were disintegrated (Fig. 9(a)) but at the output power of 50%, the structures of the membrane were significantly changed together with the formation of large pores. Accordingly, it is necessary to find the optimum operating conditions for ultrasonication by considering not only the flux recovery ratio but also the risk of membrane damage.

3.5. Comparison of the flux enhancement ratio

The flux enhancement ratios for the three physical cleaning techniques were analyzed and compared as shown in Fig. 10. It is evident that the air sparging was the most efficient to mitigate fouling under the conditions given in this study. The temperature reversal was also effective to improve flux to a certain degree. Nevertheless, special attention should be paid to apply ultrasonication due to its possibility to damage the membranes.

Based on the results in this study, the pros and cons of the each physical cleaning technique are summarized in Table 5.

4. Conclusions

In this study, fouling behaviors of the MD membranes were analyzed using different model foulants, and physical techniques including the temperature reversal, air sparging, and ultrasonication were attempted to mitigate the fouling. The following conclusions were withdrawn:

1. The foulant tendency by $CaSO_4$ was the highest and that by HA was negligible. The colloidal silica resulted in a moderate fouling.

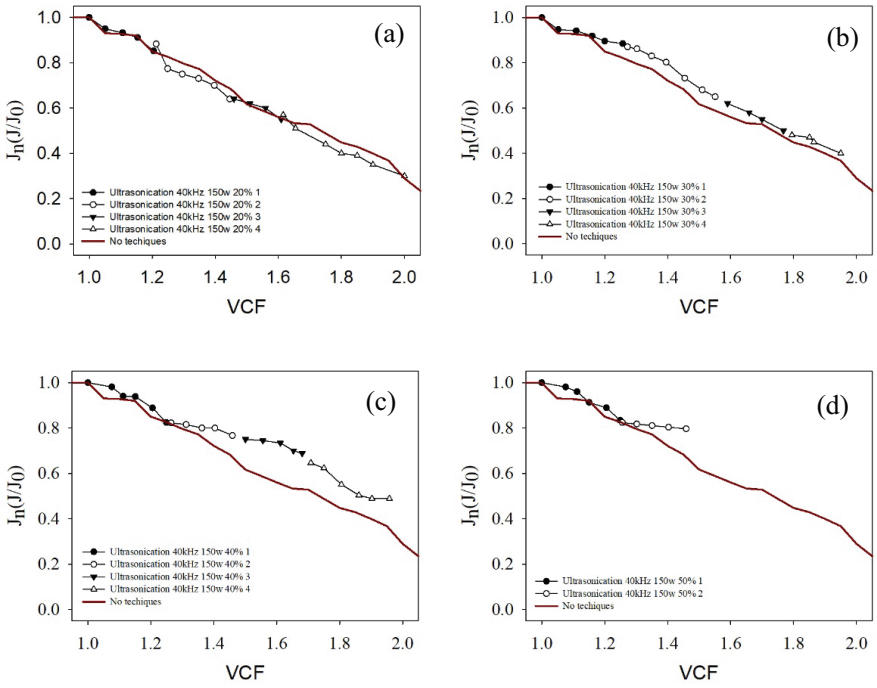

Fig. 8. Effect of ultrasonication on the normalized flux under different output power conditions (a) output power of 20%, (b) output power of 30%, (c) output power of 40%, and (d) output power of 50%.

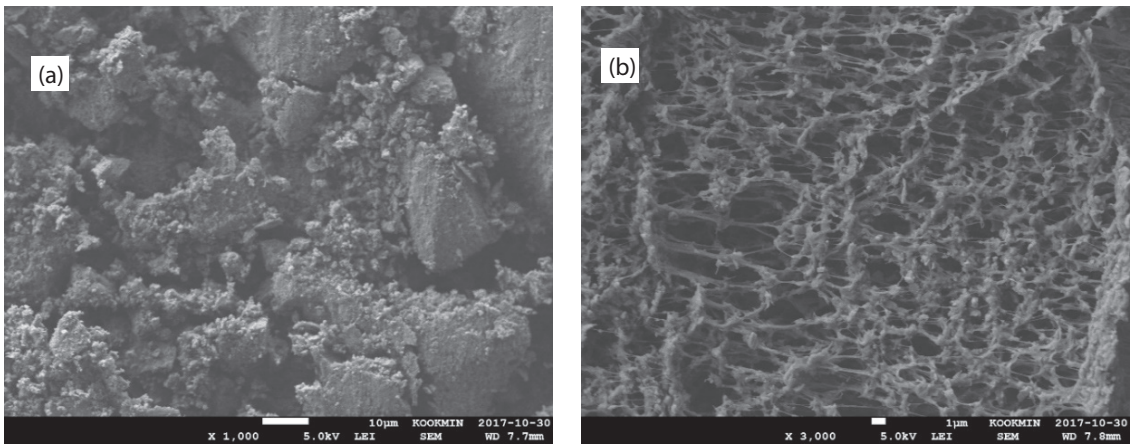

Fig. 9. FE-SEM images of the membrane after ultrasonic irradiation (a) output power of 40% and (b) output power of 50%.

Table 5
Advantages and disadvantages of the physical cleaning techniques

physical cleaning	Advantages	Disadvantages
Temperature reversal	Possibility of membrane damage at high power Periodic application of physical cleaning	Difficult to apply (immediate temperature reversal is not easy) Limited efficiency to mitigate fouling
Air sparging	Efficiency to retard fouling Relatively easy to apply Easy to control the air sparing rate	Air should be continuously supplied High electricity consumption at high air sparging rates Dissolution of air into feedwater (it may affect vapor transport rate)
Ultrasonication	Relatively easy to apply Easy to control the output power Periodic application of physical cleaning	Possibility of membrane damage at high power High electricity consumption

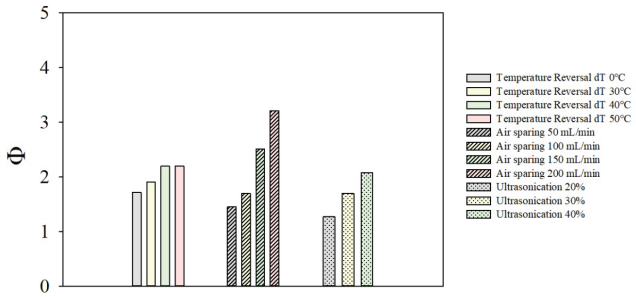

Fig. 10. Comparison of flux enhancement ratios for temperature reversal, air sparging, and ultrasonication.

2. When HA was added to the feed solutions, it generally retarded the progress of fouling. The adsorption of HA onto other foulants such as silica and $CaSO_4$ crystals seems to be the reason of this inhibition effect.
3. In the case of feed solution containing silica, HA, and $CaSO_4$, the pore blockage model showed the best fit to the experimental data ($R^2 = 0.8827$).
4. The temperature reversal was effective to improve flux to a certain degree. High difference in the temperature led to a higher recovery of flux.
5. The air sparging was more efficient to control MD fouling than the temperature reversal. As an increase in the air sparging ratio, the flux was further enhanced.
6. The ultrasonication at the output powers of 20%, 30%, and 40% resulted in the recovery of flux. However, a further increase in the output power caused the membrane damage.
7. Because the feed solution used in the physical cleaning tests simulate the compositions of wastewaters containing colloidal particles, organic matters, and inorganic salts, it is likely that the air sparging is the optimum method to control MD fouling in the treatment of such wastewaters.
8. Although physical cleaning is effective to retard MD fouling, not only physical cleaning but also chemical cleaning should be implemented. The optimum combinations of physical and chemical cleaning need to be investigated in the future.

Acknowledgement

This work is supported by the Korea Agency for Infrastructure Technology Advancement (KAIA), and the grant is funded by the Ministry of Land, Infrastructure and Transport (Grant 18FIP-B116951-03) and by Korea Ministry of Environment as "Global Top Project (2017002100001)".

References

[1] K.L. Lam, P.A. Lant, K.R. O'Brien, S.J. Kenway, Comparison of water-energy trajectories of two major regions experiencing water shortage, J. Environ. Manage., 181 (2016) 403–412.

[2] A. Ali, R.A. Tufa, F. Macedonio, E. Curcio, E. Drioli, Membrane technology in renewable-energy-driven desalination, Renewable Sustainable Energy Rev., 81 (2018) 1–21.

[3] B. Ashoor, S. Mansour, A. Giwa, V. Dufour, S. Hasan, Principles and applications of direct contact membrane distillation (DCMD): a comprehensive review, Desalination, 398 (2016) 222–246.

[4] E. Drioli, A. Ali, F. Macedonio, Membrane distillation: recent developments and perspectives, Desalination, 356 (2015) 56–84.

[5] D. González, J. Amigo, F. Suárez, Membrane distillation: perspectives for sustainable and improved desalination, Renewable Sustainable Energy Rev., 80 (2017) 238–259.

[6] P. Wang, T.-S. Chung, Recent advances in membrane distillation processes: membrane development, configuration design and application exploring, J. Membr. Sci., 474 (2015) 39–56.

[7] Z. Wang, S. Lin, Membrane fouling and wetting in membrane distillation and their mitigation by novel membranes with special wettability, Water Res., 112 (2017) 38–47.

[8] F.E. Ahmed, B.S. Lalia, R. Hashaikeh, Membrane-based detection of wetting phenomenon in direct contact membrane distillation, J. Membr. Sci., 535 (2017) 89–93.

[9] Y. Chen, M. Tian, X. Li, Y. Wang, A.K. An, J. Fang, T. He, Anti-wetting behavior of negatively charged superhydrophobic PVDF membranes in direct contact membrane distillation of emulsified wastewaters, J. Membr. Sci., 535 (2017) 230–238.

[10] M. Rezaei, D.M. Warsinger, W.M. Samhaber, Wetting prevention in membrane distillation through superhydrophobicity and recharging an air layer on the membrane surface, J. Membr. Sci., 530 (2017) 42–52.

[11] L.D. Tijing, Y.C. Woo, J.-S. Choi, S. Lee, S.-H. Kim, H.K. Shon, Fouling and its control in membrane distillation—a review, J. Membr. Sci., 475 (2015) 215–244.

[12] Q.-M. Nguyen, S. Jeong, S. Lee, Characteristics of membrane foulants at different degrees of SWRO brine concentration by membrane distillation, Desalination, 409 (2017) 7–20.

[13] J. Sanmartino, M. Khayet, M. García-Payo, H. El-Bakouri, A. Riaza, Treatment of reverse osmosis brine by direct contact membrane distillation: chemical pretreatment approach, Desalination, 420 (2017) 79–90.

[14] W. Zhong, H. Li, Y. Ye, V. Chen, Evaluation of silica fouling for coal seam gas produced water in a submerged vacuum membrane distillation system, Desalination, 393 (2016) 52–64.

[15] G. Naidu, S. Jeong, S.-J. Kim, I.S. Kim, S. Vigneswaran, Organic fouling behavior in direct contact membrane distillation, Desalination, 347 (2014) 230–239.

[16] S. Srisurichan, R. Jiraratananon, A. Fane, Humic acid fouling in the membrane distillation process, Desalination, 174 (2005) 63–72.

[17] D. Hou, Z. Wang, K. Wang, J. Wang, S. Lin, Composite membrane with electrospun multiscale-textured surface for robust oil-fouling resistance in membrane distillation, J. Membr. Sci., 546 (2018) 179–187.

[18] D.M. Warsinger, A. Servi, S. Van Belleghem, J. Gonzalez, J. Swaminathan, J. Kharraz, H.W. Chung, H.A. Arafat, K.K. Gleason, Combining air recharging and membrane superhydrophobicity for fouling prevention in membrane distillation, J. Membr. Sci., 505 (2016) 241–252.

[19] K.L. Hickenbottom, T.Y. Cath, Sustainable operation of membrane distillation for enhancement of mineral recovery from hypersaline solutions, J. Membr. Sci., 454 (2014) 426–435.

[20] D. Hou, D. Lin, C. Zhao, J. Wang, C. Fu, Control of protein (BSA) fouling by ultrasonic irradiation during membrane distillation process, Sep. Purif. Technol., 175 (2017) 287–297.

[21] G. Naidu, S. Jeong, S. Vigneswaran, Interaction of humic substances on fouling in membrane distillation for seawater desalination, Chem. Eng. J., 262 (2015) 946–957.

[22] Z. Cui, S. Chang, A. Fane, The use of gas bubbling to enhance membrane processes, J. Membr. Sci., 221 (2003) 1–35.

[23] G. Chen, X. Yang, R. Wang, A.G. Fane, Performance enhancement and scaling control with gas bubbling in direct contact membrane distillation, Desalination, 308 (2013) 47–55.

[24] D. Chen, L.K. Weavers, H.W. Walker, Ultrasonic control of ceramic membrane fouling by particles: effect of ultrasonic factors, Ultrason. Sonochem., 13 (2006) 379–387.

[25] D. Hou, L. Zhang, H. Fan, J. Wang, H. Huang, Ultrasonic irradiation control of silica fouling during membrane distillation process, Desalination, 386 (2016) 48–57.

[26] E. Iritani, N. Katagiri, Developments of blocking filtration model in membrane filtration, KONA Powder Part. J., 33 (2016) 179–202.

[27] C.Y. Tang, T. Chong, A.G. Fane, Colloidal interactions and fouling of NF and RO membranes: a review, Adv. Colloid Interface Sci., 164 (2011) 126–143.

[28] L. Han, T. Xiao, Y.Z. Tan, A.G. Fane, J.W. Chew, Contaminant rejection in the presence of humic acid by membrane distillation for surface water treatment, J. Membr. Sci., 541 (2017) 291–299.

[29] Y. Shin, J. Sohn, Mechanisms for scale formation in simultaneous membrane distillation crystallization: effect of flow rate, J. Ind. Eng. Chem., 35 (2016) 318–324.

[30] J. Benecke, J. Rozova, M. Ernst, Anti-scale effects of select organic macromolecules on gypsum bulk and surface crystallization during reverse osmosis desalination, Sep. Purif. Technol., 198 (2016) 68–78.